Stem Cell Research 61 (2022) 102785

Contents lists available at ScienceDirect

Stem Cell Research

journal homepage: www.elsevier.com/locate/scr

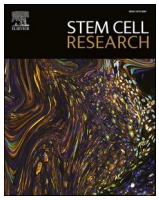

Lab Resource: Genetically-Modified Multiple Cell Lines

Generation of heterozygous (MRli003-A-5) and homozygous (MRli003-A-6) voltage-sensing knock-in human iPSC lines by CRISPR/Cas9 editing of the AAVS1 locus

Fangfang Zhang [a,b], Anna B. Meier [a,b], Daniel Sinnecker [a,b], Stefan Engelhardt [b,c], Peter Lipp [d], Karl-Ludwig Laugwitz [a,b], Tatjana Dorn [a,b], Alessandra Moretti [a,b,*]

[a] First Department of Medicine, Cardiology, Klinikum rechts der Isar, Technical University of Munich, School of Medicine & Health, Munich, Germany
[b] DZHK (German Centre for Cardiovascular Research), Partner site Munich Heart Alliance, Munich, Germany
[c] Institute of Pharmacology and Toxicology, Technical University of Munich, Munich, Germany
[d] Molecular Cell Biology, Centre for Molecular Signaling (PZMS), Medical Faculty, Saarland University, Homburg, Germany

A B S T R A C T

Assessment of the electrophysiological properties of cardiomyocytes is necessary for phenotyping cardiac disorders and for drug screening. Optical action potential imaging using a genetically encoded voltage-sensing fluorescent protein (VSFP) allows for high-throughput functional characterization of cardiomyocytes, which offers an advantage over the traditional patch-clamp technique. Here, we knocked VSFP into the *AAVS1* safe harbor locus of human iPSCs, generating two stable voltage indicator lines - one heterozygous (MRIi003-A-5) and the other homozygous (MRI003-A-6). Both lines can be used for optical membrane potential recordings and provide a powerful platform for a wide range of applications in cardiovascular biomedicine.

1. Resource table

Unique stem cell line identifier	Cell line 1: MRli003-A-5 Cell line 2: MRli003-A-6
Alternative name(s) of stem cell lines	Cell line 1: AAVS-CAG-VSFP heterozygous Cell line 2: AAVS-CAG-VSFP homozygous
Institution	Klinik und Poliklinik Innere Medizin I, Klinikum rechts der Isar – Technical University of Munich, Munich, Germany
Contact information of the reported cell line distributor	amoretti@mytum.de
Type of cell lines	iPSCs
Origin	Human, MRli003-A hiPSCs described in Moretti et al. 2020, Nature Medicine
Additional origin info	Age: N/A Sex: Male Ethnicity: Caucasian
Cell Source	Peripheral Blood Mononuclear Cell
Method of reprogramming	Non-integrating sendai virus OCT3/4, SOX2, KLF4 and MYC
Clonality	Clonal
Evidence of the reprogramming transgene loss (including genomic copy if applicable)	N/A
Cell culture system used	Essential 8™

(*continued on next column*)

(*continued*)

Type of Genetic Modification	Insertion: Cell line 1_ MRli003-A-5: with insertion of CAG-VSFP in the *AAVS1* locus in one allele Cell line 2_ MRli003-A-6: with insertion of CAG-VSFP in the *AAVS1* locus insertion in both alleles
Associated disease	N/A
Gene/locus	AAVS1 adeno-associated virus integration site 1/19q13; 19q13-qter
Method of modification/site-specific nuclease used	CRISPR/Cas9
Site-specific nuclease (SSN) delivery method	Plasmid transfection
All genetic material introduced into the cells	Cas plasmid
Analysis of the nuclease-targeted allele status	Sanger sequencing
Method of the off-target nuclease activity surveillance	Top 6 off-targets analyzed by PCR/ sequencing
Name of transgene or resistance	N/A
Eukaryotic selective agent resistance (including inducible/gene expressing cell-specific)	N/A
Inducible/constitutive system	N/A

(*continued on next page*)

* Corresponding author.
E-mail address: amoretti@mytum.de (A. Moretti).

https://doi.org/10.1016/j.scr.2022.102785
Received 14 February 2022; Received in revised form 30 March 2022; Accepted 6 April 2022
Available online 8 April 2022

(*continued*)

Date archived/stock date	14th September 2021
Cell line repository/bank	Cell line 1: https://hpscreg.eu/cell-line/MRIi003-A-5 Cell line 2: https://hpscreg.eu/cell-line/MRIi003-A-6
Ethical/GMO work approvals	The choice of appropriate human donors, the procedures for taking peripheral blood, isolation of mononuclear cells from blood, generation of iPSCs and their use in further scientific investigations were performed under the positive votes of the Ethics Committee of the Faculty of Medicine (TUM, approval number: 2109/08). All study participants gave informed consent prior to entry into the study.

2. Resource utility

Capturing action potential dynamics of cardiomyocytes is important for understanding cardiac physiology and disease. By introducing VSFP into the *AAVS1* locus, we developed a high-throughput single-cell platform for action potential recordings that facilitates disease phenotyping and drug evaluation.

3. Resource details

The voltage indicator VSFP is based on Förster resonance energy transfer (FRET) and consists of a voltage-sensing transmembrane domain fused to a pair of fluorescent proteins: Clover (GFP variant) and mRuby2 (RFP variant) (Lam et al., 2012). Depolarization of the cell membrane causes a structural rearrangement of the voltage sensor that increases the efficiency of FRET between Clover and mRuby2, allowing for optical imaging of action potentials in cardiomyocytes (Goedel et al.,

Table 1
Characterization and validation.

Classification	Test	Result	Data
Morphology	Brightfield imaging	Normal morphology	Fig. 1C, left panel
Pluripotency status evidence for the described cell line	Immunocytochemistry	OCT3/4 and NANOG staining	Fig. 1C, right panel
	Flow cytometry	TRA-1-60 (over 98% of cells positive in MRIi003-A-5 and MRIi003-A-6)	Fig. 1D
	RT-qPCR	mRNA level of *OCT3/4*, *SOX2*, *REX1*, *NANOG* and *TDGF1*	Fig. S1B
Karyotype	Karyotype (G-banding) and resolution	MRIi003-A-5: 46, XY; Resolution 450-550 bands MRIi003-A-6: 46, XY; Resolution 500–550 bands	Fig. 1F
Genotyping for the desired genomic alteration/allelic status of the gene of interest	PCR across the edited site/Sequencing	Both MRIi003-A-5 and MRIi003-A-6 determined by PCR and confirmed by Sanger sequencing	Fig. S1A
	Transgene-specific PCR	N/A	N/A
Verification of the absence of random plasmid integration events	PCR/Southern	N/A	N/A
Parental and modified cell line genetic identity evidence	STR analysis	Performed by Eurofins MWG Operon company	Supplementary file, submitted in the archive with journal
Mutagenesis/genetic modification outcome analysis	Sequencing (genomic DNA PCR or RT-PCR product)	Sanger sequencing tracks	Fig. S1A
	PCR-based analyses	Not performed	Not performed
	Western blotting (for knockouts, KOs)	Not performed	Not performed
Off-target analysis	PCR across top predicted off-target sites and sequencing	Sanger sequencing	Fig. S1D
Specific pathogen-free status	Mycoplasma	Biochemical luminescence MycoAlert™ Plus Mycoplasma Detection Kit, Lonza, Negative	Fig. S1C
Multilineage differentiation potential	Directed differentiation	Three germ layer formation: germ layer specific gene expression checked by RT-qPCR	Fig. 1E
Donor screening	HIV 1 + 2 Hepatitis B, Hepatitis C	N/A	N/A
Genotype - additional histocompatibility info	Blood group genotyping	N/A	N/A
	HLA tissue typing	N/A	N/A

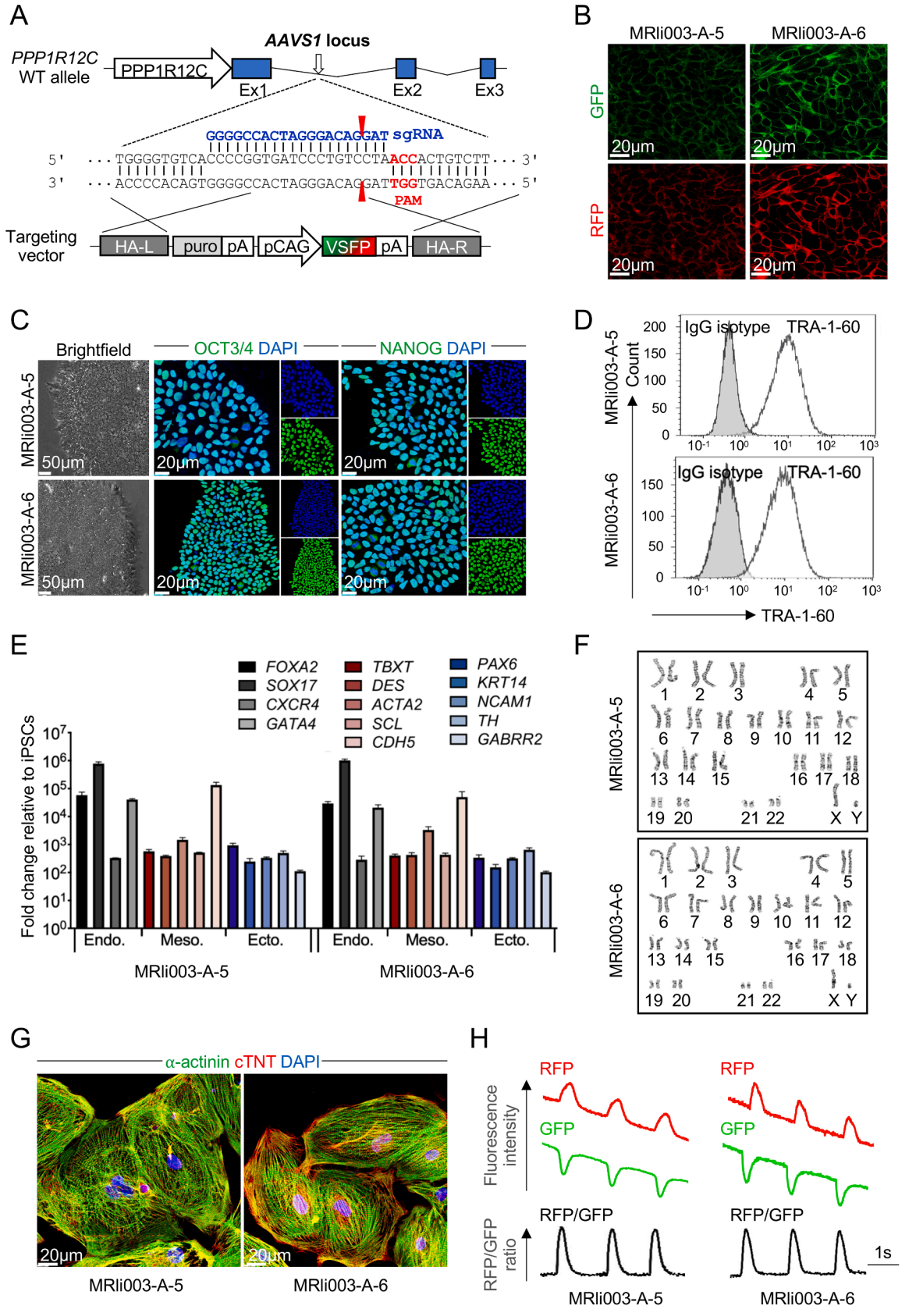

Fig. 1. Generation and validation of the AAVS1-p-CAG-VSFP knock-in iPSC lines MRIi003-A-5 and MRIi003-A-6.

Table 2
Reagents details.

Antibodies and stains used for immunocytochemistry/flow-cytometry			
	Antibody	Dilution	Company Cat # and RRID
Pluripotency markers	Rabbit anti-OCT3/4	1:200	Abcam Cat# ab19857, RRID:AB_445175) Abcam Cat# ab21624, RRID:AB_446437
	Rabbit anti-NANOG	1:200	Miltenyi Biotec Cat# 130–100-347, RRID: AB_2654227
	Human anti-TRA-1–60-PE	1:10	
Cardiomyocyte specific markers	Rabbit anti-cTNT	1:500	Abcam Cat# ab92546, RRID:AB_10585593
	Mouse anti-α-actinin	1:200	Sigma-Aldrich Cat# A7811, RRID:AB_476766
Isotype control	REA Control (S)-PE-Vio615	1:10	Miltenyi Biotec Cat# 130–107-146, RRID: AB_2661694
Secondary antibodies	Goat Anti-Rabbit Alexa Fluor 488 IgG	1:500	Invitrogen Cat# A11008, RRID:AB_143165
	Goat Anti-Mouse Alexa Fluor 594 IgG	1:500	Invitrogen Cat# A-11032, RRID:AB_2534091
Nuclear stain	Hoechst 33,258	1 μg/ml	Sigma-Aldrich Cat# 94,403
Site-specific nuclease			
Nuclease information	WT S. pyogenes Cas9 (SpCas9)	Oceguera-Yanez et al. 2016, Methods	
Delivery method	Nucleofection	Lonza; 4D-NucleofectorTM core Unit + X Unit (AAF-1002B + AAF-1002X)	
Selection/enrichment strategy	Antibiotic selection	Puromycin	
Primers and Oligonucleotides used in this study			
	Target	**Forward/Reverse primer (5′-3′)**	
Pluripotency markers	*OCT3/4*	GACAGGGGGAGGGGAGGAGCTAGG/ CTTCCCTCCAACCAGTTGCCCCAAAC	
	SOX2	GGGAAATGGGAGGGGTGCAAAAGAGG/ TTGCGTGAGTGTGGATGGGATTGGTG	
	NANOG	TGCAAGAACTCTCCAACATCCT/ATTGCTATTCTTCGGCCAGTT	
	REX1	ACCAGCACACTAGGCAAACC/TTCTGTTCACACAGGCTCCA	
	TDGF1	CCCAAGAAGTGTTCCCTGTG/ACGTGCAGACGGTGGTAGTT	
Three germ layer markers	*FOXA2*	CCGACTGGAGCAGCTACTATG/TGTACGTGTTCATGCCGTTC	
	SOX17	ACGCCGAGTTGAGCAAGA/GCGGCCGGTACTTGTAGTT	
	CXCR4	CCCTCCTGCTGACTATTCCC/TAAGGCAACCATGTGTGC	
	GATA4	GGCCTGTCATCTCACTACGG/ATGGCCAGACATCGCACT	
	TBXT	TGTTTATCCATGCTGCAATCC/CCGTTGCTCACAGACCACAG	
	DES	GTGAAGATGGCCCTGGATGT/TGGTTTCTCGGAAGTTGAGG	
	ACTA2	GTGATCACCATCGGAAATGAA/ TCATGATGCTGTTGTAGGTGGT	
	SCL	CCAACAATCGAGTGAAGAGGA/CCGGCTGTTGGTGAAGATAC	
	CDH5	CCTACCAGCCCAAAGTGTGT/TGTCCTTGTCTATTGCGGAGA	
	PAX6	CAGCTTCACCATGGCAAATAA/ATCATAACTCCGCCCATTCA	
	KRT14	CACCTCTCCTCCTCCCAGTT/ATGACCTTGGTGCGGATTT	
	NCAM1	CGACCATCCACCTCAAAGTC/CCATGGCAGTCTGGTTCTCT	
	TH	TGTACTGGTTCACGGTGGAGT/TCTCAGGCTCCTCAGACAGG	
	GABRR2	CTGTGCCTGCCAGAGTTTCA/ACGGCCTTGACGTAGGAGA	
House-Keeping genes (qPCR)	*GAPDH*	TCCTCTGACTTCAACAGCGA/GGGTCTTACTCCTTGGAGGC	
Genotyping (sequence of target region)	*AAVS1* locus sequencing after CAG-VSFP insertion	AGGAGCCCGCGTGGTTCCTG/CTGCCAAGTAGGAAAGTCCC GTTCATAGCCCATATATGGAG/AGGCTTTCACGCAGCCACAG TGACTGACCGCGTTACTCCC/CTGAACCGTCGAATCCCTCC TTGGCAAAGAATTCCTCGAGG/ CCCTTGCTCACCATTCGACG TCGTTGTCACATTCGTCGTC/CAGGTAGTGGTTGTCGGGCA AACCGCATCGAGCTGAAGG/CTGCGTGTTCGCGTTGTACT AGTTGATGGTGGTGGCCATC/CCTCTCCTGGGCTTGCCAAG	
Donor construct cloning	bGH-polyA amplifying primer	GCATTTAATTAACCAGTGTGGTGGAATTCTGCAGATATC/ CCGGGTCGACCCATAGAGCCCACCGCATCCCCAGCAT G	
Targeted mutation analysis/sequencing	Sequencing data from both alleles	N/A	
Potential random integration-detecting PCRs	e.g. plasmid backbone, for targeting events- vector/ homology arm end PCRs	N/A	
sgRNA oligonucleotide	*AAVS1* locus specific	GGGGCCACTAGGGACAGGAT	
Oligo for cloning sgRNA	N/A	N/A	
Genomic target sequence(s)	*AAVS1* locus	AAVS1 adeno-associated virus integration site 1/19q13; 19q13-qter	
Top off-target mutagenesis predicted site sequencing (for CRISPR/Cas9)	*SNORA25-AL603632.1*	CTAACTATGAAGCCTTGAGTAAC/ GAGCAGTATAATGAATGCAC	
	DAPK2-RP11-111E14.1	CACAGAGACATGTCTCTTTGTG/ GACAATGGCACATCTGATCCAG	
	RNU6-715P-RNA5SP106	GAGATGAAGACTCCAATTTAG/ CACTAATGATGTTCACTCAACAG	
	RP11-93L14.1-CTNNA3	CACTCACACACCTCACCAAGAC/ GTTCTTGGAGAGCCATTTATTTC	
	OR1AB1P-CTD-2231E14.4	TCAACTACCTTATTCTCCTGAG/ ACTAGCTGCATGACCCCATCAG	
	AC006041.1-RP11-196O16.1	ACATATAGCCAGAGCACAAC/TGTGTTGATAGCATAGGTAGCs	

2018). Here, we used CRISPR/Cas9 technology to knock *VSFP* into one or both alleles of the *AAVS1* locus of an iPSC line derived from a healthy male (MRIi003-A) (See Table 1).

We targeted the *AAVS1* safe harbor locus with a single guide RNA (sgRNA) and a donor vector containing the CAG promoter-driven VSFP reporter flanked by the left and right *AAVS1* homology arms (HA-L, HA-R) (Fig. 1A). After editing, sequencing showed that CAG-VSFP was successfully inserted into the *AAVS1* locus, either in one allele (MRIi003-A-5 line) or both (MRIi003-A-6 line) (Fig. S1A). Both lines expressed Clover and mRuby2 and as expected the intensity of the reporter signal was stronger in the homozygous MRIi003-A-6 iPSCs than in the heterozygous MRIi003-A-5 iPSCs (Fig. 1B).

Both lines formed typical iPSC colonies positive for the pluripotency markers OCT3/4 and NANOG (MRIi003-A-5: passage 16, MRIi003-A-6: passage 16, Fig. 1C). Quantitative real-time PCR (qRT-PCR) also confirmed that their mRNA expression levels of *OCT3/4*, *SOX2*, *REX1*, *NANOG,* and *TDGF1* were significantly higher than in fibroblasts (MRIi003-A-5: passage 16, MRIi003-A-6: passage 16, Fig. S1B). Moreover, over 98% of cells of both lines expressed the surface pluripotency marker TRA-1-60 (MRIi003-A-5: passage 17, MRIi003-A-2: passage 18, Fig. 1D), as analyzed by flow cytometry. Successful differentiation into the three germ layers was validated by qRT-PCR analysis of markers of endoderm (*FOXA2*, *SOX17*, *CXCR4,* and *GATA4*), mesoderm (*TBXT*, *DES*, *ACTA2*, *SCL,* and *CDH5*) and ectoderm (*PAX6*, *KRT14*, *NCAM1*, *TH,* and *GABRR2*) (MRIi003-A-5: passage 16, MRIi003-A-6: passage 16, Fig. 1E).

Importantly, both lines exhibited a normal karyotype after editing (MRIi003-A-5: passage 10, MRIi003-A-6: passage 8, Fig. 1F) and no mutations were detected at the six intergenic loci with the highest off-target editing scores for the sgRNA used (Fig. S1D). Of note, no mutations in the coding regions within the first 30 off-targets with the highest scores have been predicted for this sgRNA. Mycoplasma testing showed no contamination (Fig. S1C).

Finally, we applied a Wnt-based cardiac differentiation protocol to both lines (Foo et al., 2018) and efficiently generated $cTNT^{+}$ α-$actinin^{+}$ cardiomyocytes (Fig. 1G). Importantly, we could image changes in RFP and GFP fluorescence intensities in spontaneously contracting two months-old cardiomyocytes derived from both MRIi003-A-5 and MRIi003-A-6 iPSCs. By calculating the RFP/GFP signal ratio, we could record action potentials (Fig. 1H), making these lines suitable models for investigating cardiac physiology.

4. Materials and methods

4.1. iPSC culture

iPSCs were cultured on Geltrex-coated (Thermo Fisher Scientific, A14133-02) plates in Essential 8 (Thermo Fisher Scientific, A1517001) containing 0.5% Penicillin/Streptomycin (Thermo Fisher Scientific, 15140–122) at 37 °C, 5% CO_2. Cells were passaged at a ratio of 1:14 every 4–5 days using 0.5 mM EDTA (Thermo Fisher Scientific, AM9260G). After passaging, the medium was supplemented with 10 μM Thiazovivin (Sigma-Aldrich, SML1045) for 24 h.

4.2. Cloning of donor constructs

To construct the donor plasmid pAAVS1-p-CAG-VSFP-polyA, the pcDNA3.1/Puro-CAG-VSFP-CR plasmid (Addgene #40257) was digested with SpeI and CAG-VSFP was cloned into the pAAVS1-p-MCS vector (Addgene #80488), which was digested with SpeI. Then, the bovine growth hormone polyadenylation (bGH-polyA) signal was amplified by PCR from the pcDNA3.1/Puro-CAG-VSFP-CR plasmid using primers containing PacI- at 5′ and SalI-restriction sites at 3′ and introduced into the pAAVS1-p-CAG-VSFP, digested with PacI and SalI.

4.3. 4D nucleofection of iPSCs

For editing, 10^6 iPSCs were nucleofected with 1 μg pXAT2 plasmid containing the *AAVS1* locus-specific sgRNA (Oceguera-Yanez et al., 2016; Addgene #80494) and 3 μg donor construct (pAAVS1-p-CAG-VSFP-polyA) following the Lonza Amaxa 4D Nucleofector basic protocol for human stem cells before reseeding in Matrigel-coated (BD, 354277) 24 well-plates in mTeSR1 (Stemcell Technologies, 05854) containing 10 μM Thiazovivin. 24 h after nucleofection, mTeSR1 medium was replaced without Thiazovivin. 48 h later, 0.2 μg/ml puromycin (Calbiochem, 540411) was added for 7 days. When colonies were large enough, cells were dissociated with Accutase (Thermo Fisher Scientific, A11105-01) and replated for single clone expansion.

4.4. Immunocytochemistry

Immunocytochemistry was performed as previously described (Dorn et al., 2018) with the antibodies listed in Table 2.

5. Flow cytometry

iPSCs were dissociated with Accutase and 10^6 cells were stained with TRA-1-60-PE or the corresponding isotype antibody (Table 2). Data were acquired at a Gallios flow cytometer (Beckman Coulter, Germany) and analyzed with Kaluza software version 1.2.

6. Quantitative real-time PCR (qRT-PCR)

RNA isolation, cDNA synthesis and qRT-PCR were performed as previously described (Dorn et al., 2018). Gene expression levels were normalized to *GAPDH*. The primers used for qRT-PCR are listed in Table 2.

7. Mycoplasma detection

Mycoplasma detection was performed with the MycoAlert PLUS Mycoplasma Detection Kit (Lonza, LT07-703).

8. Genotyping

The genotype of the clones was determined by PCR followed by Sanger sequencing (Eurofins MWG Operon) (primers listed in Table 2).

9. Karyotyping

Karyotyping was performed at the Institute of Human Genetics of the Technical University of Munich via metaphase preparation and G-banding ($\geq$20 metaphases counted).

10. Trilineage differentiation

Cells were differentiated into the three germ layers in 2D using the StemMACS™ Trilineage Differentiation Kit (Miltenyi Biotec, 130–115-660) according to manufacturer's instructions.

11. STR analysis

STR analysis was performed by Eurofins MWG Operon.

12. Off-target analysis

Potential off-target sites were predicted using CRISPOR (https://crispor.tefor.net). Top sequences were amplified (primers are listed in Table 2) and verified by Sanger sequencing.

13. Differentiation towards cardiomyocytes

iPSCs were differentiated towards cardiomyocytes as described in Foo et al. 2018.

14. Optical membrane potential recordings

Membrane potential measurements were performed as described in Goedel et al. 2018.

Declaration of Competing Interest

The authors declare that they have no known competing financial interests or personal relationships that could have appeared to influence the work reported in this paper.

Acknowledgements

We thank Birgit Campbell and Christina Scherb for their technical assistance in cell culture and molecular cloning and Gabi Lederer (Cytogenetic Department, TUM) for karyotyping. This work was supported by grants from: the European Research Council (ERC), (788381 to A.M.); the German Research Foundation, Transregio Research Unit 152 (to A.M., K-L.L., and P.L.) and 267 (to A.M., K-L.L. and S.E.); the German Centre for Cardiovascular Research (DZHK), (FKZ 81Z0600601 to A.M. and K-L.L.), (FKZ 81X2600608 to A.M. and P.L).

Appendix A. Supplementary data

Supplementary data to this article can be found online at https://doi.org/10.1016/j.scr.2022.102785.

References

Dorn, T., Kornherr, J., Parrotta, E.I., Zawada, D., Ayetey, H., Santamaria, G., Iop, L., Mastantuono, E., Sinnecker, D., Goedel, A., et al., 2018. Interplay of cell–cell contacts and RhoA/MRTF-A signaling regulates cardiomyocyte identity. EMBO J. 37, e98133.

Foo, K.S., Lehtinen, M.L., Leung, C.Y., Lian, X., Xu, J., Keung, W., Geng, L., Kolstad, T.R., Thams, S., Wong, A.O., et al., 2018. Human ISL1+ Ventricular Progenitors Self-Assemble into an In Vivo Functional Heart Patch and Preserve Cardiac Function Post Infarction. Mol. Ther. 26, 1644–1659.

Goedel, A., Zawada, D.M., Zhang, F., Chen, Z., Moretti, A., Sinnecker, D., 2018. Subtype-specific optical action potential recordings in human induced pluripotent stem cell-derived ventricular cardiomyocytes. J. Vis. Exp. 2018.

Lam, A.J., St-Pierre, F., Gong, Y., Marshall, J.D., Cranfill, P.J., Baird, M.A., McKeown, M. R., Wiedenmann, J., Davidson, M.W., Schnitzer, M.J., Tsien, R.Y., Lin, M.Z., 2012. Improving FRET dynamic range with bright green and red fluorescent proteins. Nat Methods 9 (10), 1005–1012.

Oceguera-Yanez, F., Kim, S.-I., Matsumoto, T., Tan, G.W., Xiang, L., Hatani, T., Kondo, T., Ikeya, M., Yoshida, Y., Inoue, H., Woltjen, K., 2016. Engineering the AAVS1 locus for consistent and scalable transgene expression in human iPSCs and their differentiated derivatives. Methods 101, 43–55.